Journal of the Korean Electrochemical Society
Vol. 2, No. 3, 1999, 163-170

A Simulated Prediction for Influences of Operating Condition in an Alkaline Fuel Cell

Jang-Ho Jo† and Sung-Chul Yi

Department of Chemical Engineering, Hanyang University, Seoul 133-791, Korea

(Received June 22, 1999 : Accepted July 19, 1999)

Abstract

The effects of the operating conditions in AFC single cells have not been studied in detail. In this study, by using a one-dimensional isothermal model a computational simulation was conducted to investigate the effects of the initial electrolyte concentration and the operating gas pressure. According to the result, the optimum electrolyte concentration at the base-case was found to be within 3.0~3.5 M. The variation of the cell performance according to the electrolyte concentration was found to be caused mainly by the charge transfer resistances of both electrodes, Henry's constant and the liquid phase diffusivity of the dissolved gases. It was also found that an increase in operating pressure increased the reaction rates and the solubilities of the gases, which led to a considerable enhancement of the cell performance.

초 록 : AFC 단전지에서 운전조건의 영향은 이제까지 자세히 연구된 바 없다. 본 연구에서는 초기 전해질 농도와 가스 운전압력의 영향을 살펴보기 위하여 1차원 등온 모델을 이용해 전산모사를 수행하였다. 결과에 의하면, base-case에서 최적 전해질 농도는 3.0~3.5 M 사이에 있는 것으로 발견되었다. 전해질 농도에 따른 전지 성능의 변화는 주로 양쪽 전극의 전하전달 저항과 용해된 기체의 헨리상수 및 액상확산이 원인인 것으로 밝혀졌다. 또한, 운전 압력의 증가는 반응속도와 가스의 용해도를 증가시켰으며, 이것으로 인해 전지 성능이 상당히 향상되는 것으로 조사되었다.

Key words : Mathematical modeling, AFC, Single cell, Electrolyte concentration, Operating pressure

1. Introduction

Operating conditions such as temperature, pressure and electrolyte concentration, of a fuel cell considerably affect the cell performance. AFCs (alkaline fuel cell) are also affected by the operating conditions. Although there have been several experimental and simulation studies to find out the influences of such operating conditions on a single electrode of AFC,[1,2] the influences in AFC single cell were hardly known in detail. Thus, an investigation on the effects of the operating condition was conducted by using the one-dimensional model developed from our previous work[3] where Orbiter Fuel Cell of IFC (International Fuel Cell Corp.) was considered as a base-case model. Operating temperature was excluded in this study since the model is an isothermal one.

The investigation on the influences of the operating conditions on the cell polarization could be performed by experiments relatively with ease. However, the reasons for a performance variation, an interaction between the electrodes or other changes in condition within the cell are technically difficult to be investigated by the experiment alone because of the complexity of the phenomena in the AFC or the limitation of the experimental equipment, etc. A prediction by using a mathematical model can help solve such problems. By using the simulation, it is possible not only to obtain the predicted cell polarization, but also to investigate the reason for the changes in the cell performance.

It is generally known that the optimum electrolyte concentration is 6~7 M in AFC systems and a deviation from this value lowers the cell performance. However, detailed effects of the electrolyte concentration on an AFC single cell have not been known. It is expected that the initial electrolyte concentration has a significant and complicated effects, since the most thermodynamic, transport and electrochemical properties of the reactants in AFCs are functions of the electrolyte concentration.

Increasing the operating pressure is well known to have a positive effect on the performance of AFCs.[4] However, like the case of the electrolyte concentration, the detailed investigation of the effects in AFC single cells is not readily available in open literature.

In this study, we predicted the changes in the cell performance as the operating condition was varied, and the reasons for such changes were also investigated intensively.

2. Description of the System

The AFC single cell considered in this study consists of five layers, which are anode gas-diffusion layer, anode cata-

†E-mail: janghojo@hymail.hanyang.ac.kr

lyst layer, separator layer, cathode catalyst layer and cathode gas-diffusion layer. A schematic diagram of the cell is illustrated in Fig. 1.

In the anode catalyst layer, dissolved hydrogen reacts electrochemically with hydroxide ions on anode catalyst surfaces.

$$H_2 + 2OH^- \rightarrow 2H_2O + 2e^- \quad (1)$$

The electron generated from the above reaction leaves the cell, then goes toward the cathode.

In the cathode catalyst layer, dissolved oxygen reacts electrochemically with water by the following reaction,

$$O_2 + 2H_2O + 4e^- \rightarrow 4OH^- \quad (2)$$

The hydroxide ion produced from the above reaction penetrates the separator, then reaches the anode catalyst layer.

According to the hydrogen oxidation (1) and oxygen reduction (2), the overall reaction in an AFC is given by

$$H_1 + \frac{1}{2}O_2 \rightarrow H_2O \quad (3)$$

Detailed descriptions of the model and the phenomena in an AFC were introduced in our previous work.[3)]

3. Mathematical Modeling

Each layer of the cell was considered as homogeneous continuum. Such an assumption is based on the macroscopic model of Newman and Tiedemann.[5)]

The equation of continuity for species i can be written in the general form for a porous medium as

$$\frac{\partial \varepsilon C_i}{\partial t} = -\nabla N_i + R_i^p + R_i^e \quad (4)$$

where ε is porosity, t is time and C_i, N_i refer to the concentration and molar flux of species i, respectively. R_i^p and R_i^e indicate mass transfer rate across a phase boundary and electrochemical reaction rate of species i per unit volume of the electrode, respectively.

In a gas phase, Stefan-Maxwell equation can be employed for N_i,

$$\nabla y_i = \sum_j \frac{RT}{P\mathcal{D}_{ij}^g}(y_i N_j^g - y_j N_j^g) \quad (5)$$

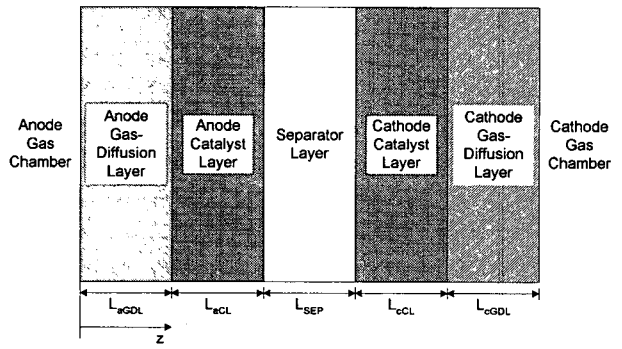

Fig. 1. Schematic diagram of an AFC single cell.

where R is gas constant, T is temperature, P is total pressure and superscript g indicates gas phase. y_i and $\mathcal{D}_{ij}^g$ refer to gas phase mole fraction of species i and gas phase effective diffusivity of species i in j, respectively.

In liquid phase, Nernst-Plank equation can be employed for N_i,

$$N_i^l = -\mathcal{D}_i^l \nabla C_i - z_i \omega_i F C_i \nabla \Phi - C_i v \quad (6)$$

where F is Faraday's constant and Φ is solution phase potential. $\mathcal{D}_i^l$, z_i and ω_i^g indicate liquid phase effective diffusivity, charge number and effective mobility of species i, respectively. The superscript l refers to liquid phase. The effective diffusivity $\mathcal{D}_i^g$ is related with free stream diffusivity D_i, porosity ε and tortuosity τ as following,

$$\mathcal{D}_i = \frac{\varepsilon D_i}{\tau} \quad (7)$$

Similarly, effective mobility ω_i can be expressed as

$$\omega_i = \frac{\varepsilon^l u_i}{\tau^l} \quad (8)$$

If an equilibrium is assumed at a gas-electrolyte interface, the mass transfer rate across the phase boundary R^p_i can be approximately described as following,

$$R_i^p = -a^g D_i^l \left(\frac{H_i P_i - C_i}{\delta}\right) \quad (9)$$

where a^g is specific area of gas-electrolyte interface, H_i is Henry's law constant of species i, and δ is thickness of electrolyte film. In the above equation, the minus sign at the front of a^g indicates that species i goes out across a phase boundary. Hence, if species i come into current phase from the other, this sign will be converted into plus.

The electrochemical reaction rate per unit volume R^e_i can be represented as following,

$$R_i^e = \frac{s_i a^l i}{nF} \quad (10)$$

where a^l is specific area of catalyst-electrolyte interface, and n is number of electrons transferred. The stoichiometric coefficient of species i s_i is given by expressing an electrochemical reaction in the form

$$\sum_i s_i M_i^{z_i} \rightarrow ne^- \quad (11)$$

The local current density i is described by Butler-Volmer electrochemical reaction rate expression,

$$i = i_o\left[\prod_i \left(\frac{C_i}{C_i^r}\right)^{q_i} \exp\left(\frac{\alpha_a F\eta}{RT}\right) - \prod_j \left(\frac{C_j}{C_j^r}\right)^{q_j} \exp\left(-\frac{\alpha_c F\eta}{RT}\right)\right] \quad (12)$$

where i_o is exchange current density, C^r_i is concentration of species i at a reference condition, q_i is reaction order of species i. α_a and α_c are apparent anodic and cathodic transfer coefficient, respectively. The local overpotential η is given by

$$\eta = E - \Phi - U \quad (13)$$

where E is the electrical potential at electrically conductive solid phase, and U is theoretical open-circuit potential at given concentrations. U is given by

$$U = U^{\theta} - \frac{RT}{nF}\sum_{i} s_i \ln\left(\frac{C_i}{C_i^{\theta}}\right) \quad (14)$$

where U^{θ} is theoretical open-circuit potential evaluated at standard concentrations C_i^{θ} and temperature T.

In a porous electrical conductive medium, ohmic drop can be described by Ohm's law.

$$\nabla E = -\frac{I}{\sigma} \quad (15)$$

where I is total current density. The effective electrical conductivity σ is related with bulk electrical conductivity κ volume fraction of electrically conductive solid phase ε^s and tortuosity of the phase τ^s as following

$$\sigma = \frac{\varepsilon^s \kappa}{\tau^s} \quad (16)$$

ε^s is associated with ε^g, ε^l and volume fraction of PTFE ε^{TF} as following

$$\varepsilon^g + \varepsilon^l + \varepsilon^s + \varepsilon^{TF} = 1 \quad (17)$$

These general equations presented above were employed to describe each layer.

4. Model Parameters and Operating Condition

All of the base-case model parameters and correlations used in the present study can be found in our previous work,[3] and some of the parameters are listed in Table 1.

Orbiter Fuel Cells which is considered as the base-case model in this study, are operated typically at 80°C and 4.1 atm with 7 M KOH solution. Hence, these were considered as the base-case operating condition in this work and are listed in Table 2. The operating conditions were varied within a pertinent range to obtain predicted cell polarizations. Both total pressures of the anode and cathode gas-diffusion layers were set to the operating gas pressure to avoid an overflow of the gaseous gases across the separator.

Table 1. Values of important base-case parameters

parameter (unit)	gas-diffusion layers	catalyst layers	separator layer
L (cm)	0.025	0.005 (anode) 0.010 (cathode)	0.005
ε^g	0.7	0.1	
ε^l		0.6	0.8
ε^s	0.2	0.2	
t	1.2	1.2	1.0
a^g (cm^{-1})		7.0×10^3	
a^l (cm^{-1})		2.4×10^5	
δ (cm)		5.0×10^{-5}	
i_o (A/cm^2)		5.0×10^{-4}(anode) 5.0×10^{-8}(cathode)	

Table 2. Base-case operating condition

parameter	value (unit)
C_e^r	7.0 (M)
T	80 (°C)
P_a^r	4.1 (atm)
P_c^r	4.1 (atm)

5. Method of Solution

The model developed in our previous work consists of total 11 variables, 25 governing equations and 38 inner and outer boundary conditions. The model equations are highly coupled and nonlinear thus a numerical solution is necessary. The governing equations and boundary conditions were discretized by using second-order and first-order finite difference schemes, respectively. The resulting finite difference approximations have a banded matrix structure and it was solved by Newman's BAND algorithm.[6]

6. Results and Discussions

6.1. Influence of Initial Electrolyte Concentration

Since most thermodynamic, transport and electrochemical properties of the reactants are functions of the electrolyte concentration C_e, a variation in the initial electrolyte concentration C_e^r could have large effects on the cell performance. For instance, an increase in C_e decreases the gas solubility and the partial pressure of water vapor P_w. It also enhances the hydrogen oxidation kinetic but diminishes the oxygen reduction rate as expected from Eq. (1) and (2). Hence, the variation in C_e^r would lead to very complicated phenomena.

Fig. 2 illustrates the influence of C_e^r on the cell polarization. As shown in Fig. 2, by lowering C_e^r the performance is enhanced in the ohmic and concentration polarization region except the case of 1 M. On the other hand, the current density I in the active polarization region steadily increases with the lowering of C_e^r. Such a tendency can be seen clearly in Fig. 3. In this figure, it is shown that diluting the electrolyte from 6 M to 4 M dramatically increases I at a low cell volt-

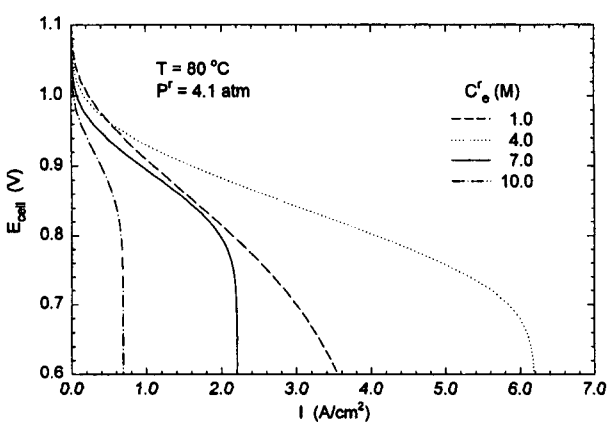

Fig. 2. Influence of initial electrolyte concentration on the polarization of the AFC.

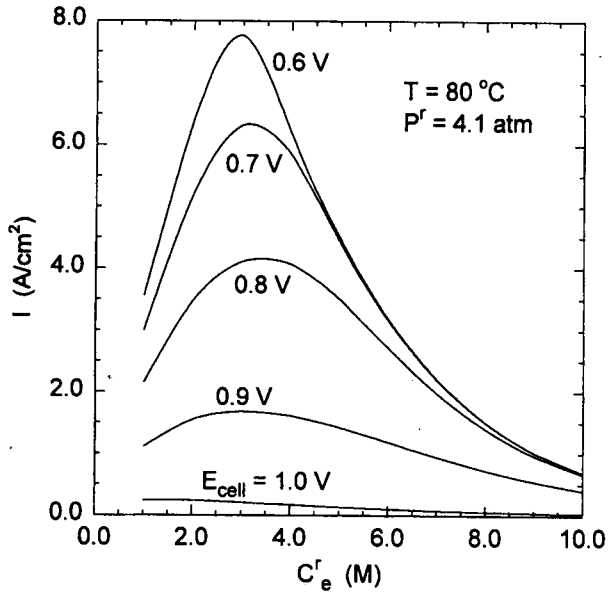

Fig. 3. Current density as a function of initial electrolyte concentration for several cell voltages.

age, however, diluting the electrolyte below 3 M reduces I to a large extent. The optimum C_e^r is also found to be between 3.0 M~3.5 M except the case of 1.0 V. These values are considerably different from well known value 6 M~7 M which is used mostly in common AFC systems. KOH solution at the concentration between 6 M~7 M is used due to a maximum ionic conductivity at this concentration[4] as shown in Fig. 4. The ionic conductivity κ_e shown in Fig. 4 was calculated by using the following correlation[7] which was used in our model.[3]

$$\kappa_e = \frac{5.6106C_e(79.931 - 3673.9C_e)}{(1.0016 + 37.205C_e)^2} \quad (18)$$

The experimental data on the effects of C_e^r on the performance in an AFC single cell are not readily available, however, it has been reported that the electrolyte concentration at the highest performance of Raney nickel hydrogen electrode is ca. 4 M as studied by Kenjo.[1] Although the different electrode and operating pressure were used, this value is similar to that of the present study. Thus it is considered that the concentration of 6 M~7 M, which is commonly used in many AFC systems, may not be an optimum value. Simultaneously, it should be noted that low electrolyte concentration could yield some problems such as flooding of the catalyst layer or difficulty in water management due to an increase in P_w. Since these problems are, however, beyond the scope of this work, they were not considered in this study.

Distinct influences of C_e^r on the polarization curves are an increase in I_L and a reduction of the slope in the ohmic polarization region R_{ohm} with a dilution of the electrolyte beyond 4 M, as mentioned above. The increase in I_L is attributed to increase in Henry's constant of oxygen H_O, which results in an increase in oxygen solubility H_OP_O, and the liquid phase diffusivity of oxygen D_O^l, not those of hydrogen. Note that in the present AFC model the rate determining step at I_L exists in the cathode, not in the anode, as shown in our previous work.[3] H_O at a constant pressure and D_O^l increase exponentially with a decrease in C_e,[8-11] thus I_L increases exponentially with the decrease in C_e^r.

Fig. 5 shows the influence of C_e^r on R_{ohm}. In the figure, it can be seen that R_{ohm} decreases with a decrease in C_e^r at the high concentration. However, the decrease of R_{ohm} in the range of 4 M~7 M is not readily comprehensible because κ_e decreases with the decrease of C_e in the range, as shown in Fig. 4. Hence, the decrease in R_{ohm} is questionable.

In order to investigate whether there is a decease in the ionic resistance of the cell with a decrease in C_e^r within 4 M ~7 M in spite of the decrease in κ_e, the potential drop in the electrolyte $\Delta\Phi$ throughout the catalyst layers and separator were calculated at I of 1.0 A/cm^2. The calculation showed

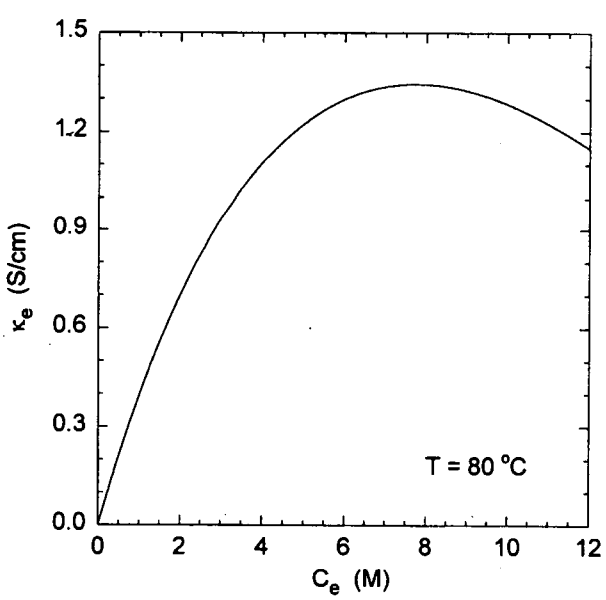

Fig. 4. Ionic conductivity of KOH solution as a function of the conentration.

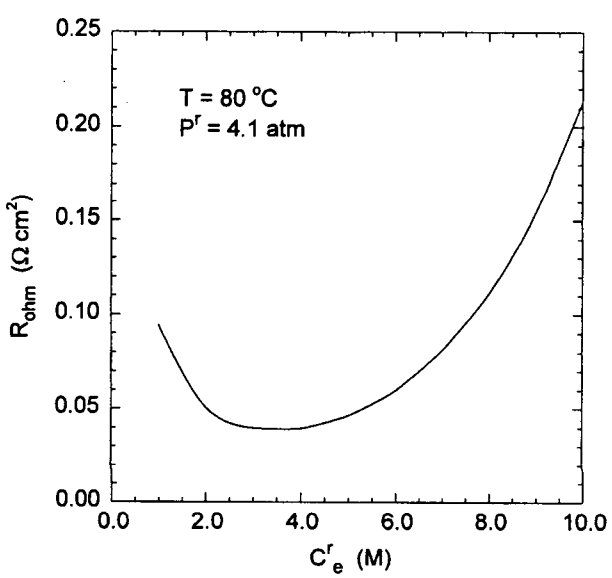

Fig. 5. The slope of ohmic polarization region as a function of the electrolyte concentration.

that $\Delta\Phi$ were 11.4 mV and 13.2 mV at C_e^r of 7 M and 4 M, respectively. Obviously, decreasing C_e^r seems to increase $\Delta\Phi$ as expected in Fig. 4. Therefore, it is concluded that the decrease in R_{ohm} is not caused by the ionic resistance. Additionally, the decrease in R_{ohm} is not attributed to the electrical resistance in the cell since the electrical resistance is independent of C_e^r.

As mentioned above, lowering C_e^r lead to an increase of I_L. This implies that a decrease in the liquid phase diffusional resistance of the dissolved gases occurs with the lowering of C_e^r. The decrease in the diffusional resistance could yield the decrease in R_{ohm}, since the diffusional resistance is known to contribute to R_{ohm} to a certain extent.[12] In Fig. 6, it can be seen that the decrease in C_e^r from 7 M to 4 M makes the concentration of the dissolved hydrogen C_H and that of the dissolved oxygen C_O about three times higher. Such large increases in C_H and C_O represents clearly the decrease in the liquid phase diffusional resistance. Therefore, the decrease in R_{ohm} seems to be affected by the decrease in liquid phase diffusional resistances of the dissolved gases.

Another possible reason for the decrease of R_{ohm} is the influence of C_e^r on the electrochemical reaction rates, since the charge transfer resistance of electrode is known to affect R_{ohm}.[12] As expected from Eq. (1) and (2), a lowering of C_e^r enhances the charge transfer rate of oxygen reduction, but decreases that of hydrogen oxidation. These imply that as the electrolyte is diluted the charge transfer resistance of the cathode decreases and that of the anode increases. In the case of 1.0 V in Fig. 3, it could be confirmed that the charge transfer resistance of the cathode is reduced with the lowering of C_e^r. Note that E_{cell} of 1.0 V corresponds to the activation polarization region where the charge transfer resistance of the cathode is dominant. Hence, the decrease of R_{ohm} is partly due to the decrease in the charge transfer resistance of the cathode.

Consequently, the decrease of R_{ohm} with the decrease of C_e^r within 4 M~7 M is considered to result from the decreases of the liquid phase diffusional resistances of the dissolved gases and from the decrease of the charge transfer resistance of the cathode.

A decrease of the performance with the lowering of C_e^r below 4 M can be observed in Fig. 3 and 5, in spite of the increase of C_H and C_O as shown in Fig. 6. Two reasons could be considered for such phenomenon.

As shown in Fig. 4, diluting the electrolyte below 4 M diminishes κ_e. Hence, diluting the electrolyte would increase the ionic resistance of the cell. According to our calculation, $\Delta\Phi$ throughout the catalyst layers and separator layer were 13.2 mV and 34.2 mV at C_e^r of 4 M and 1 M, respectively, when I was 1.0 A/cm^2. Thus the increase in the ionic resistance is considered to decrease the cell performance.

The other reason that caused the decrease in the performance was the use of the electrolyte having low concentration which has an unfavorable effect on the hydrogen oxidation at the anode. Fig. 7 illustrates the distribution of the open-circuit potential of the anode U_a and that of the cathode U_c as a function of C_e^r. Despite the increase of C_H

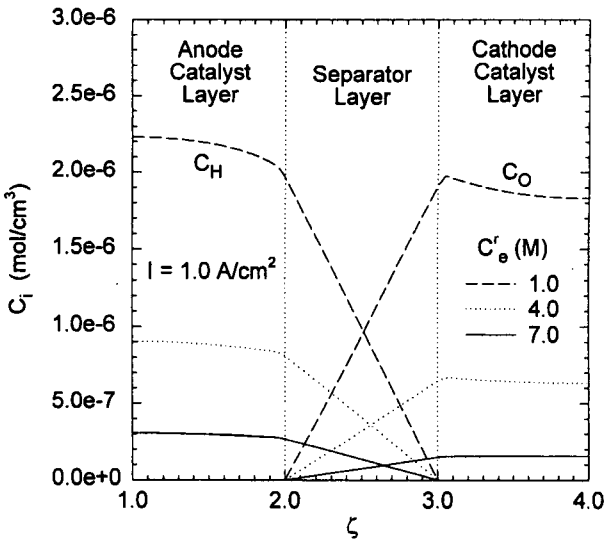

Fig. 6. Distribution of the dissolved gases as a function of the electrolyte concentration.

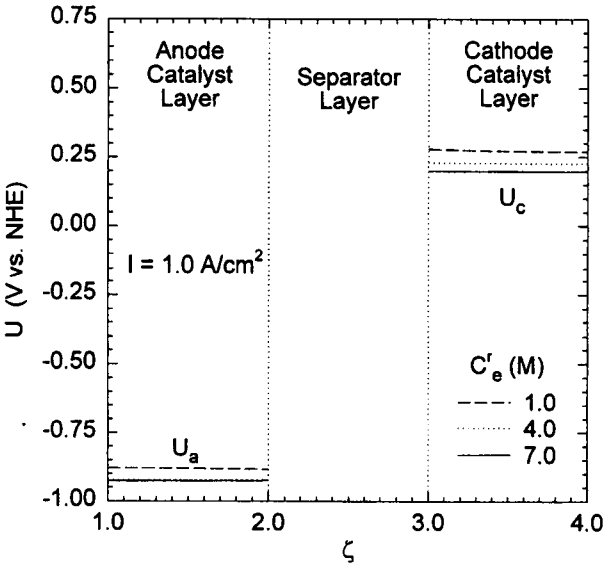

Fig. 7. Distribution of open-circuit potential as a function of the electrolyte concentration.

and C_O with the decrease of C_e^r as shown in Fig. 6, an increase of U_a, which is unfavorable to the hydrogen oxidation, is observed in Fig. 7. If the increases of C_H and Nernst equation are taken into account, it is evident that the increase in U_a is attributed to the extremely low C_e^r. Hence, it is concluded that the lower C_e^r creates greater charge transfer resistance of the anode, then the greater resistance contributes to the increase of R_{ohm}.

Consequently, it is considered that decreasing C_e^r below 4 M causes increases in the ionic resistance of the cell and in charge transfer resistance of the anode, then these lead to the decrease in the cell performance.

6.2. Influence of Operating Pressure

Fig. 8 shows the polarization curves as a function of the operating gas pressure P^r. An enhancement of the cell perfor-

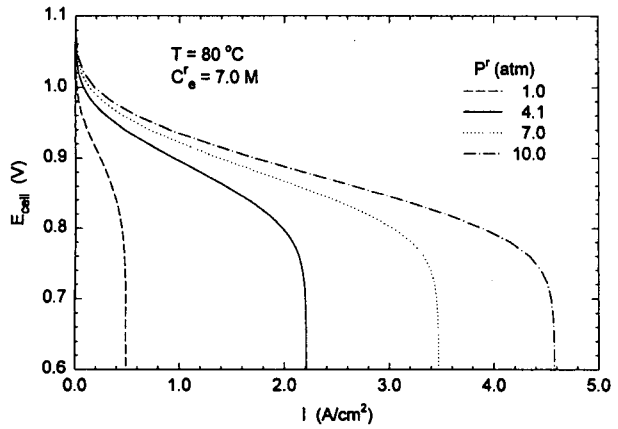

Fig. 8. Influence of operating pressure on the polarization of the AFC.

mance with increasing P^r is observed in the figure, as generally known. In particular, an increase in I_L and a decrease in R_{ohm} are noticeable.

The I_L could be increased by an increase in the liquid phase diffusivity or the solubility of the reactant gases. The solubility H_iP_i is composed of Henry's constant H_i and partial pressure of the gas P_i, and H_i and D^l_i are functions of C_e. According to our analysis, there is no change in C_e distribution throughout the cell with increasing P^r at a constant I. Thus H_i and D^l_i of the gases remain constant with increasing P^r. Moreover, since no changes in the electrode structure which could affect I_L was assumed in this study, any influences by the structural parameter were absent. Therefore, it is concluded that the increase of I_L is caused solely by the increase of P_H and P_O due to the increasing P^r.

R_{ohm} as a function of P^r is represented in Fig. 9. As shown in the figure, at low pressure a small increase in P^r decreases R_{ohm} considerably, while, at high pressure even a large increase in P^r causes only a small variation in R_{ohm}. Hence, it is considered that P^r has a larger effect on R_{ohm} at low P^r than at high P^r.

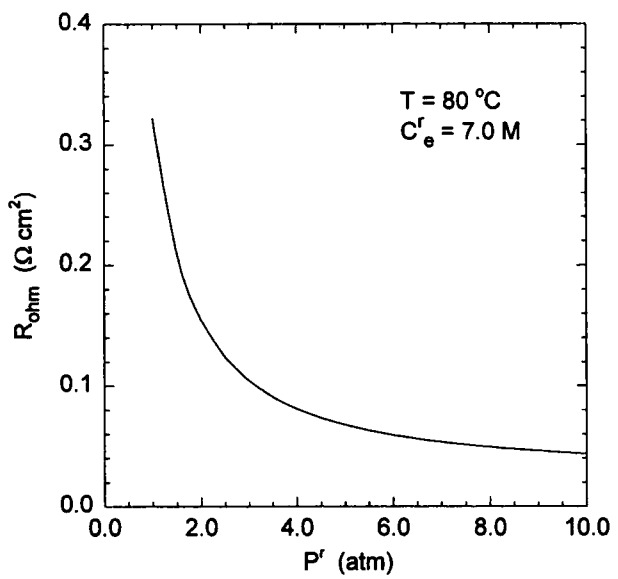

Fig. 9. The slope ohmic polarization region as a function of operating pressure.

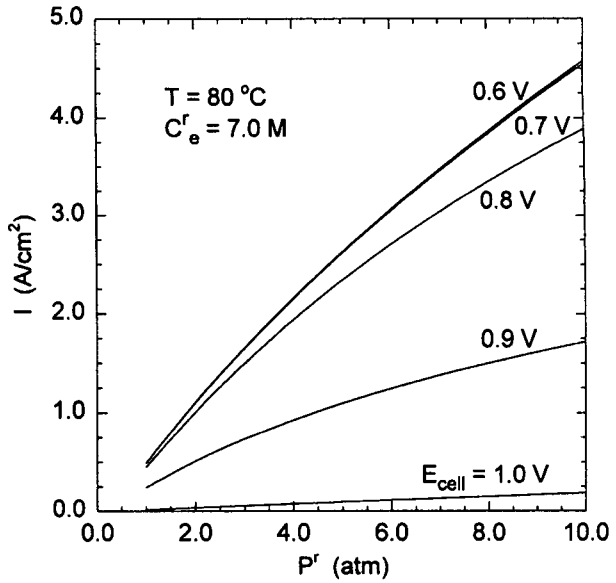

Fig. 10. Current density as a function of operating pressure for several cell voltages.

As mentioned in the previous section, R_{ohm} could be affected by ionic or electrical resistance, charge transfer resistance and liquid phase diffusional resistance.[12] Hence, all these factors could be considered as reasons for the decrease of R_{ohm} with increasing P^r. In order to investigate the influence of the ionic resistance, $\Delta\Phi$ throughout the catalyst layers and separator layer were calculated in P^r range of 1 to 10 atm at a constant I. According to the calculation, $\Delta\Phi$ was not changed at all during the variation of P^r. Additionally, note that the electrical resistance is not a function of P^r. Hence the ionic or electrical resistance are not responsible for the decrease of R_{ohm} with the increasing P^r. An increase in P^r the pressure allows faster charge transfer rate as well known, and such effect can be confirmed from the case of 1.0 V in Fig. 10. It should be also noted that R_{ohm} decreases with an increase in I_L, as mentioned in the previous section. Therefore, the decrease of R_{ohm} is considered to be caused by the decrease in the charge transfer resistances and by the increase in the gas solubilities due to increasing P_i of the gases.

7. Conclusions

Influences of the operating condition in the AFC single cell were investigated. Through the investigation, it was found that the initial electrolyte concentration had an optimum of 3.0 M~3.5 M when the cell voltage is between 0.6 V~0.9 V. Whereas, the current density at 1.0 V increased steadily as the electrolyte concentration decreased. The increase of the limiting current density with the lowering of the electrolyte concentration was found to be due to the increase in Henry's constant and the liquid phase diffusivity of the dissolved gases. It was also considered that the major factors affecting the slope of the ohmic polarization region in the electrolyte concentration of 4 M~7 M were the charge

transfer resistances of the cathode and the liquid phase diffusional resistance of the dissolved gases. On the other hand, in the electrolyte concentration below 4 M, the slope was considered to be affected mainly by the charge transfer resistance of the anode and the ionic resistance of the electrolyte.

The partial pressures of reactant gases were found to be the only cause for the increase in the limiting current density with increasing the operating pressure. The decrease of the slope at the ohmic polarization region with the increasing pressure was considered to be caused by the enhancement of the charge transfer rate at both electrodes and by the increases of the gas solubilities.

Acknowledgment

This paper was partially supported by CPRC (Ceramic Processing Research Center) of Hanyang University, Korea. The authors deeply appreciate the support.

List of Symbols

a^g : specific area of gas-electrolyte interface (cm^2/cm^3)
a^l : specific area of catalyst-electrolyte interface (cm^2/cm^3)
C_i : concentration of species i (mol/cm^3)
D_i : free stream diffusivity of species i (cm^2/sec)
$\mathcal{D}_i$: effective diffusivity of species i (cm^2/sec)
E : electrical potential of electrode (V)
E_{cell} : applied single cell voltage (V)
F : Faraday constant (=96485.309 C/mol)
H_i : Henry's constant of species ($mol/cm^3 \cdot atm$)
I : current density of single cell (A/cm^2)
I_L : limiting current density of single cell (A/cm^2)
i : local current density (A/cm^2)
i_o : exchange current density (A/cm^2)
L : thickness of layer (cm)
M_i : molecular weight of species i (mg/mol)
N_i : molar flux of species i ($mol/cm^2 \cdot sec$)
n : number of electron transferred
P_i : partial pressure of species i (atm)
q_i : reaction order of species i
R : ideal gas constant (=8.31451 J/mol·K)
R^e_i : electrochemical reaction rate of species i ($mol/cm^3 \cdot sec$)
R^p_i : mass transfer rate of species i across phase boundary ($mol/cm^3 \cdot sec$)
R_{ohm} : slope of polarization curve in ohmic polarization region ($\Omega \cdot cm^2$)
s_i : stoichiometric coefficient of species i
T : temperature (K)
t : time (sec)
U : open-circuit potential (V vs. NHE)
u_i : mobility of species i ($mol \cdot cm^2/J \cdot sec$)
$\mathcal{u}_i$: effective mobility of species i ($mol \cdot cm^2/J \cdot sec$)
$v^{\blacksquare}$: volume average velocity (cm/sec)
y_i : vapor phase mole fraction of species i
z : spatial coordinate (cm)
z_i : charge number of species i

Greek

α_a : apparent anodic transfer coefficient
α_c : apparent cathodic transfer coefficient
δ : thickness of electrolyte film (cm)
ε : porosity
ζ : dimensionless spatial coordinate
η : local overpotential (V)
κ : electrical conductivity (S/cm)
κ_e : ionic conductivity of electrolyte (S/cm)
σ : effective electrical conductivity (S/cm)
τ : tortuosity
Φ : solution phase potential (V)

Superscripts

a : anode
c : cathode
g : gas phase
l : liquid phase
e : electrochemical reaction
r : reference condition
p : mass transfer across a phase boundary
TF : PTFE
s : electrically conductive solid phase
θ : standard condition

Subscripts

a : anode
c : cathode
CL : catalyst layer
aCL : anode catalyst layer
cCL : cathode catalyst layer
e : electrolyte
GDL : gas-diffusion layer
aGDL: anode gas-diffusion layer
cGDL: cathode gas-diffusion layer
H : H_2
i : species i
j : species j
O : O_2
SEP : separator layer
w : H_2O
+ : cation(K^+)
– : anion(OH^-)

References

1. T. Kenjo, *J. Electrochem. Soc.*, **133**, 2051 (1986).
2. S. M. A. Shibli and M. Noel, *J. Power Sources*, **45**, 139 (1993).
3. J. -H. Jo and S. -C. Yi, *J. Power Sources*, Accepted (1999).
4. H. van den Broeck, in *Fuel Cell Systems*, L. J. M. J. Blomen, M.N. Mugerwa, Editor, p.250, p.42, Plenum Press, New York (1993).
5. J. Newman and W. Tiedemann, *AIChE J.*, **21**, 25 (1975).
6. J. Newman, *Ind. Eng. Chem. Fundam.*, **7**, 514 (1968).
7. A. L. Horvath, Handbook of Aqueous Electrolyte Solutions: Physical Properties, Estimation and Correlation Methods, 252, Ellis Horwood, Ltd., Chichester, England (1985).

8. P. Ruetschi and R. F. Amile, *J. Phys. Chem.*, **70**, 718 (1966).
9. S. K. Shoor, R. D. Walker, Jr. and K. E. Gubbins, *J. Phys. Chem.*, **73**, 312 (1969).
10. M. K. Tham, R. D. Walker and K. E. Gubbins, *J. Phys. Chem.*, **74**, 1747 (1970).
11. R. E. Davis, G. L. Horvath and C. W. Tobias, *Electrochim. Acta*, **12**, 287 (1967).
12. S. Srinivasan, D. J. Manko, H. Koch, M. A. Enayetullah and A. J. Appleby, *J. Power Sources*, **29**, 367 (1993).